Supplementary Information

Spin light-emitting devices in a 2D magnet

Fanglu Qin[§], Haiyang Liu[§], Aosai Yang, Yilin Liu, Xuanji Wang, Yue Sun, Xinyi Zhou, Zdenek Sofer, Jiayuan Zhou, Xue Liu, Sheng Liu[*], Vanessa Li Zhang, Xiaoze Liu*, Weibo Gao, Ting Yu[*]

Table of Contents

Section I: **Layer-by-layer Assembly and Device Integration.**

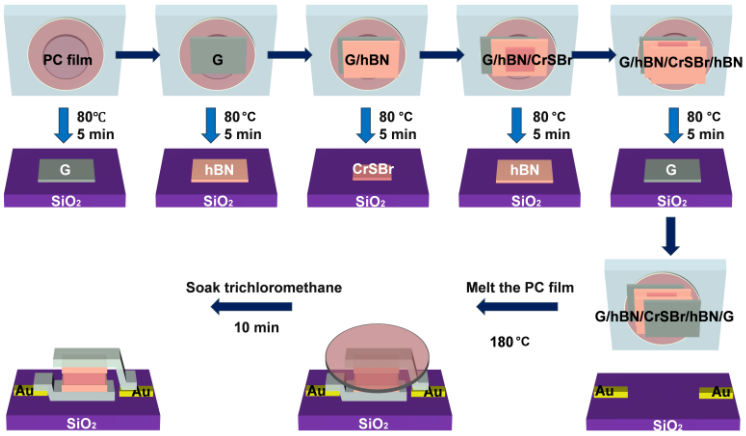

Figure S1. Fabrication process of the CrSBr QW device.

The Graphite/hBN/CrSBr/hBN/Graphite heterostructure is assembled using sequential pickup with a PDMS/PC stamp at 80 °C (5 min per layer). The stack was subsequently transferred onto pre-patterned electrodes by softening the PC at 180 °C, followed by immersion in trichloromethane ($CHCl_3$) for 10 minutes to remove residual polymer.

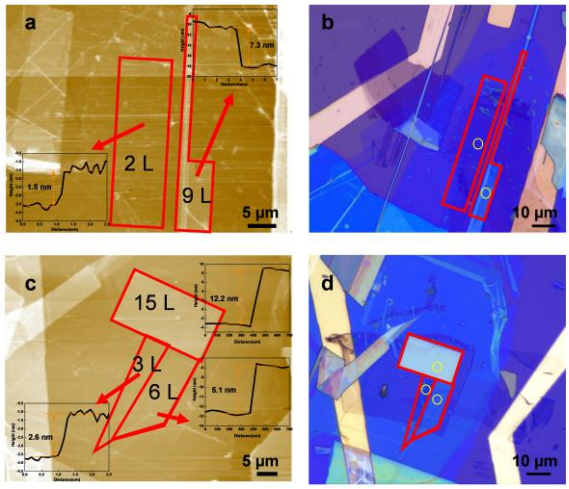

Figure S2. AFM (a) and optical microscope (b) images of CrSBr QW device, with measured heights of 1.5 nm and 7.3 nm corresponding to the 2-layer and 9-layer CrSBr regions, respectively. AFM (c) and optical microscope (d) images of CrSBr QW device, showing regions with measured heights of 2.6 nm, 5.1 nm, and 12.2 nm, corresponding to 3-layer, 6-layer, and 15-layer CrSBr, respectively. Yellow circles indicate test positions.

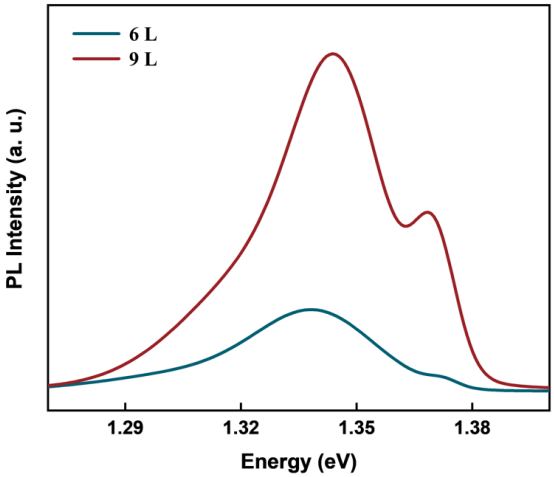

Figure S3. PL spectra of 6-layer and 9-layer CrSBr.

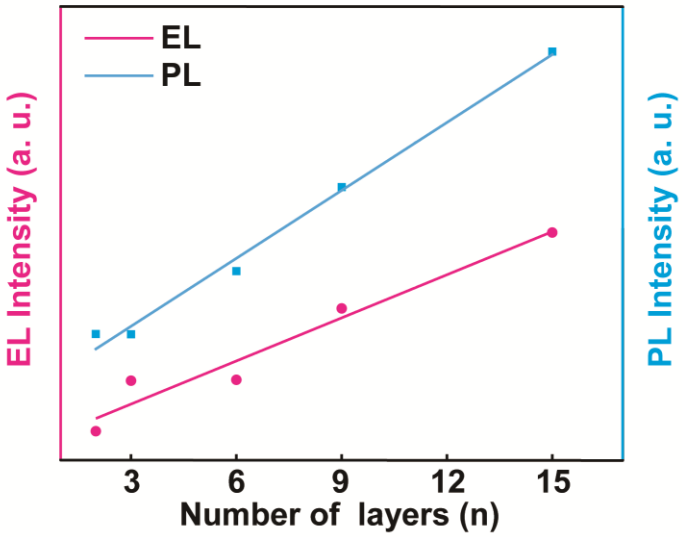

Figure S4. Layer-dependent PL and EL intensity of X_s in CrSBr.

Section II: QW Device Characteristics

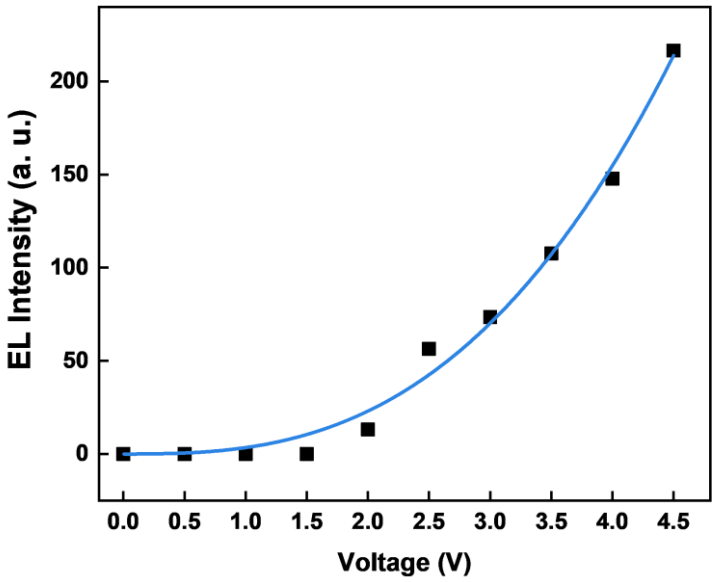

Figure S5. Voltage-dependent EL intensity of 15-layer CrSBr QW device at 2 K.

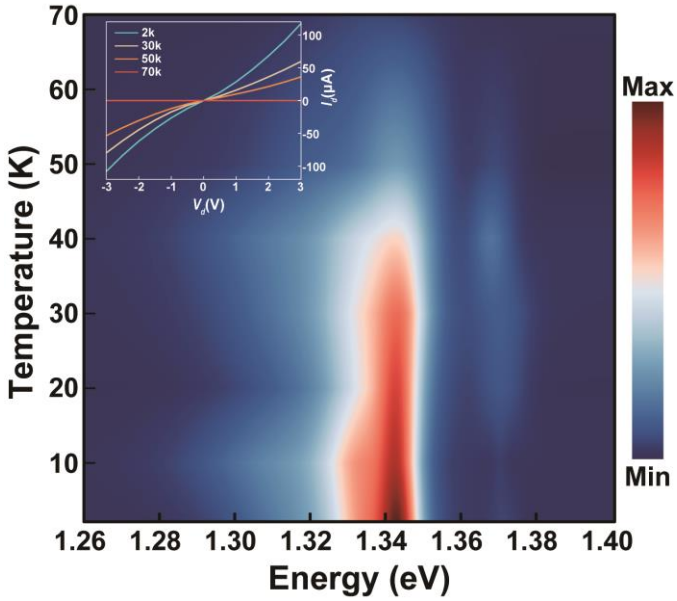

Figure S6. EL spectra of 15-layer CrSBr measured over the temperature range of 2 K to 70 K. Inset: temperature-dependent *I-V* curve across the same temperature range.

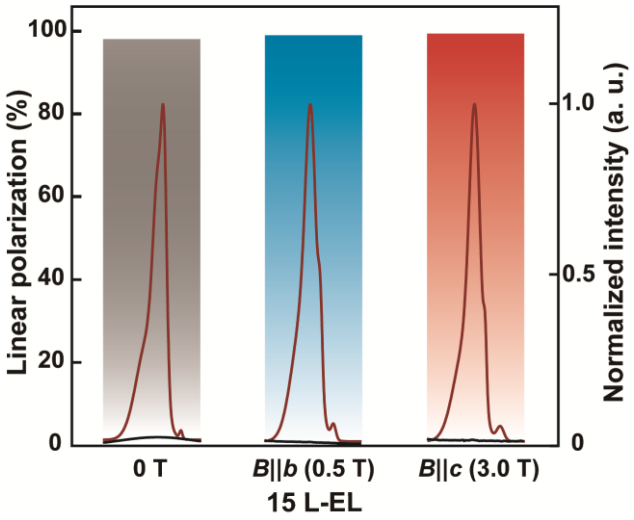

Figure S7. Calculated EL linear polarization ratio (ρ) (colar bars) and normalized intensity at 0° (red lines) and 90° (dark lines) for 15-layer CrSBr under 0 T, 0.5 T (in-plane), 3 T (out-of-plane) *B*.

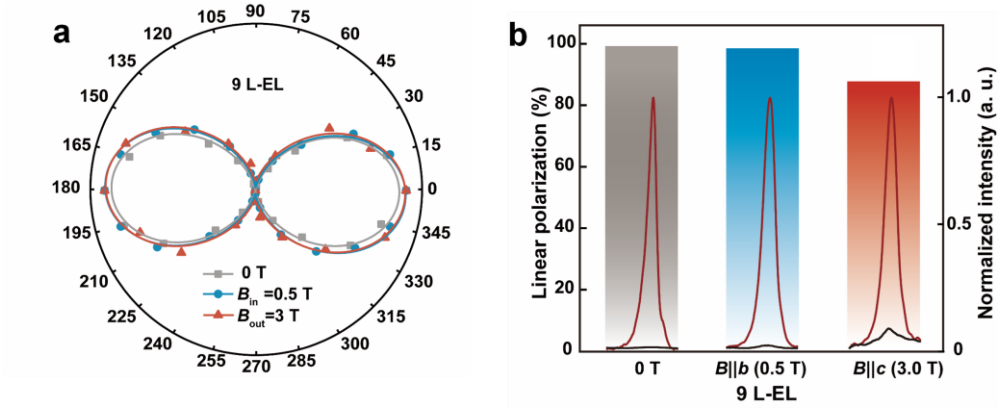

Figure S8. (a) Linear polarization of EL as polar plot for 9-layer CrSBr under 0 T, 0.5 T (in-plane), 3 T (out-of-plane) *B*. Experimental data are represented by dots, solid curves correspond to fitting results. (b) Calculated EL linear polarization ratio (ρ) and normalized intensity at (red lines) 0° and 90° (dark lines) for 9-layer CrSBr under 0 T, 0.5 T (in-plane), 3 T (out-of-plane) *B*.

Section III: In-Plane Magnetic Field Control of EL and PL in CrSBr.

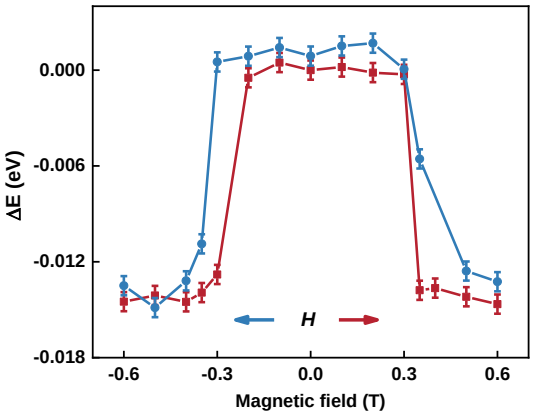

Figure S9. Difference in EL energy shift of X_b during a back-and-forth sweep of *B* for 15-layer CrSBr, where 0 T is referenced to 0 eV.

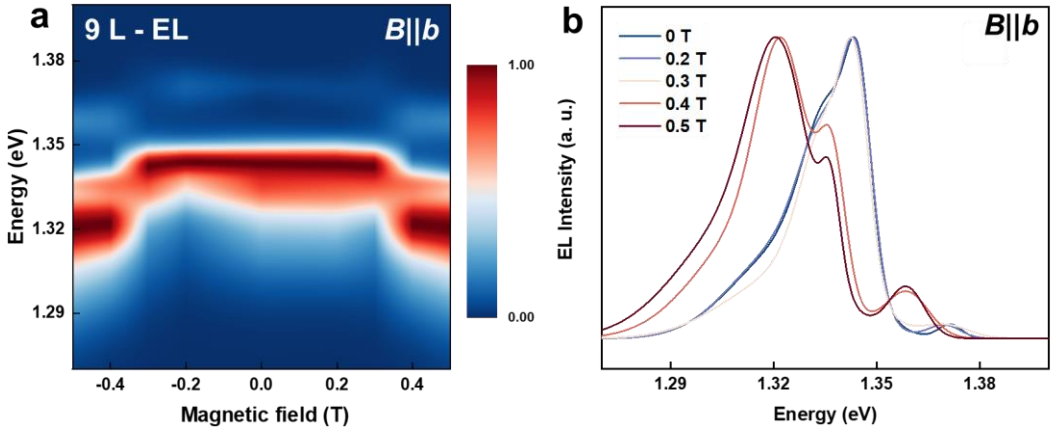

Figure S10. (a) EL spectra of 9-layer CrSBr as magnetic field is swept along the easy axis from -0.5 to 0.5 T. (b) EL spectra of 9-layer CrSBr under five different magnetic fields.

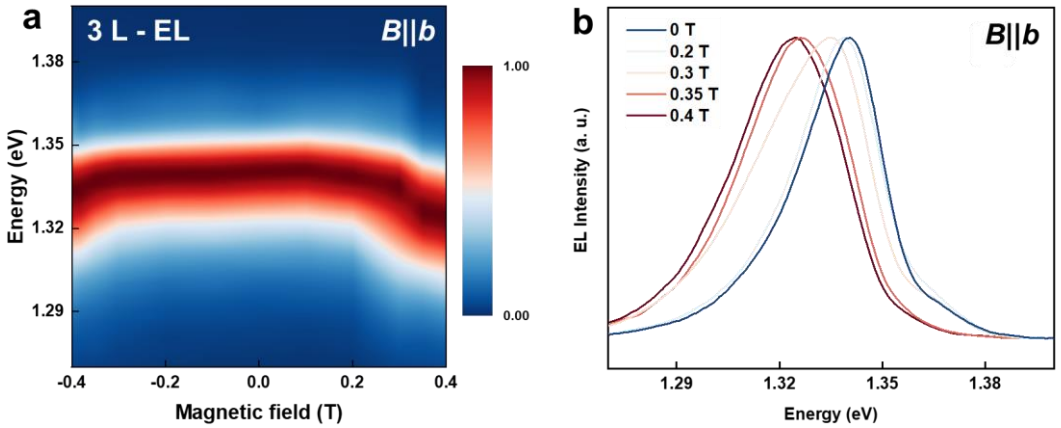

Figure S11. (a) EL spectra of 3-layer CrSBr as magnetic field is swept along the easy axis from -0.4 to 0.4 T. (b) EL spectra of 3-layer CrSBr under five different magnetic fields.

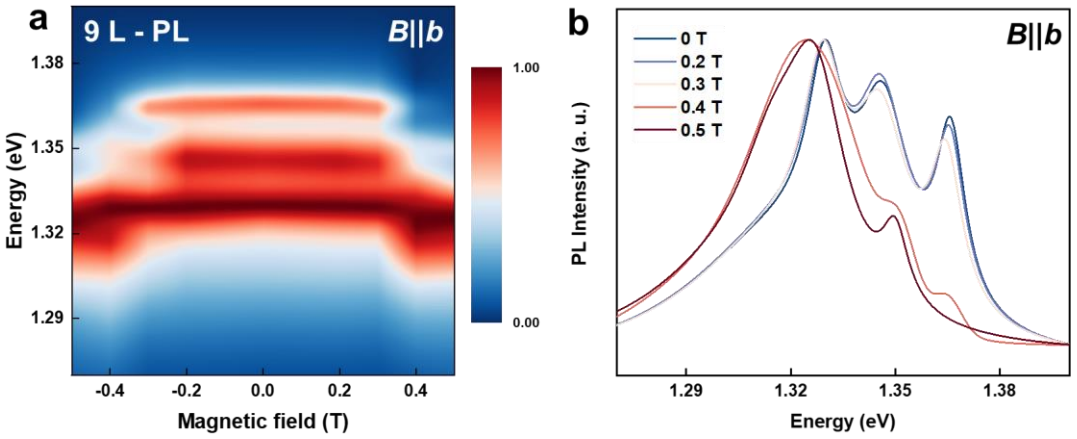

Figure S12. (a) PL spectra of 9-layer CrSBr as magnetic field is swept along the easy axis from -0.5 to 0.5 T. (b) PL spectra of 9-layer CrSBr under five different magnetic fields.

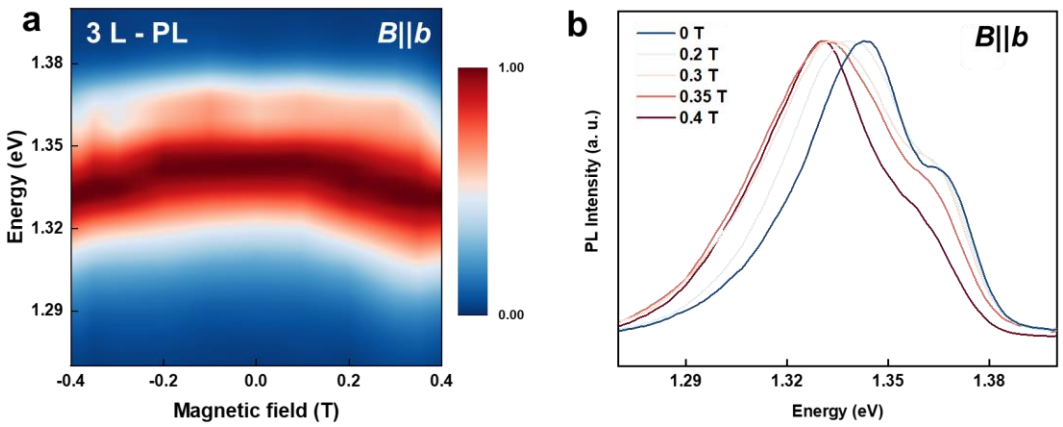

Figure S13. (a) PL spectra of 3-layer CrSBr as magnetic field is swept along the easy axis from -0.4 to 0.4 T. (b) PL spectra of 3-layer CrSBr under five different magnetic fields.

To quantify the modulation efficiency of EL by magnetic orders, we define the modulation efficiency (η) as the change in the relative EL intensity (I) under an applied B_{in}:

$$\eta_{in} = \frac{I_B - I_0}{I_0} \times 100\%,$$

where E_B and I_0 represent the EL intensities with and without the E, respectively. When B_{in} applied along the b-axis is increased from 0 T to 0.6 T, a modulation efficiency η_{in} of 48.9% is achieved. This modulation efficiency is comparable to or even exceeds that of established magnetically controlled OLEDs[1-3], demonstrating the potential of this system as an opto-spintronic device for multiple applications, such as a high-speed magnetic field sensor with an opto-coupler, a magnetic field visualizer, or an optical readout device for magnetoresistive random-access memory (MRAM).

Section IV: Out-of-Plane Magnetic Field Control of EL and PL in CrSBr.

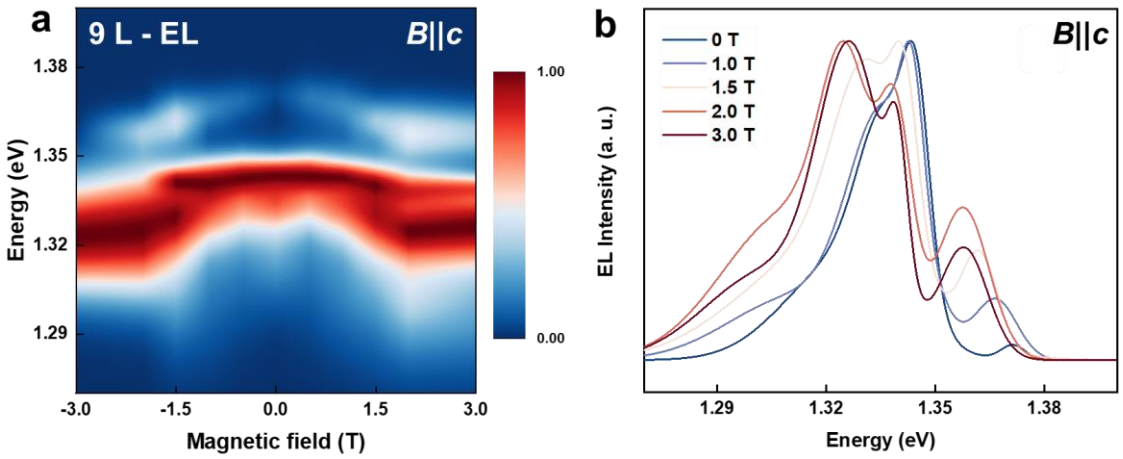

Figure S14. (a) EL spectra of 9-layer CrSBr as magnetic field is swept along the hard axis from -3 to 3 T. (b) EL spectra of 9-layer CrSBr under five different magnetic fields.

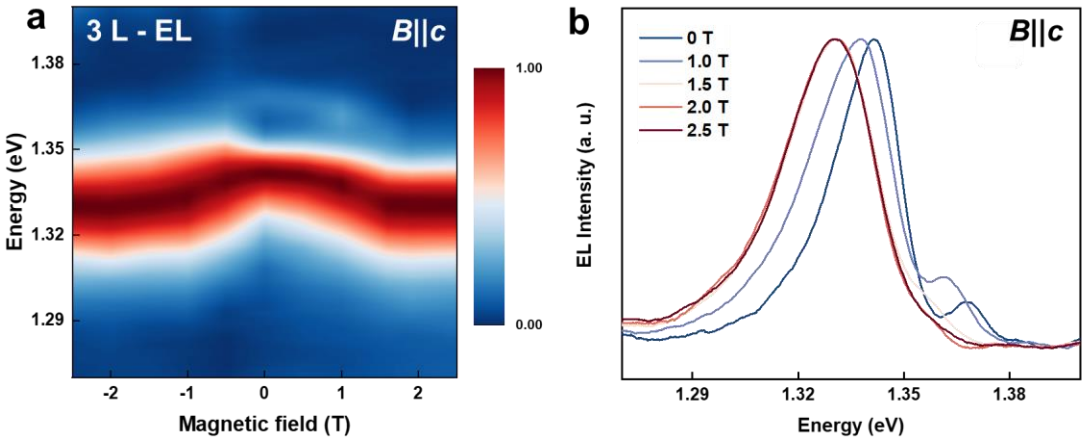

Figure S15. (a) EL spectra of 3-layer CrSBr as magnetic field is swept along the hard axis from -2.5 to 2.5 T. (b) EL spectra of 3-layer CrSBr under five different magnetic fields.

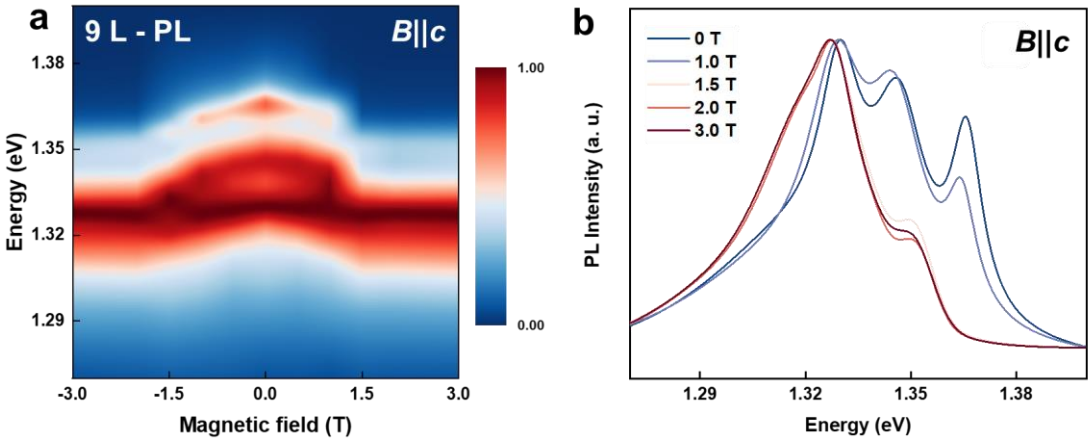

Figure S16. (a) PL spectra of 9-layer CrSBr as magnetic field is swept along the hard axis from -3 to 3 T. (b) PL spectra of 9-layer CrSBr under five different magnetic fields.

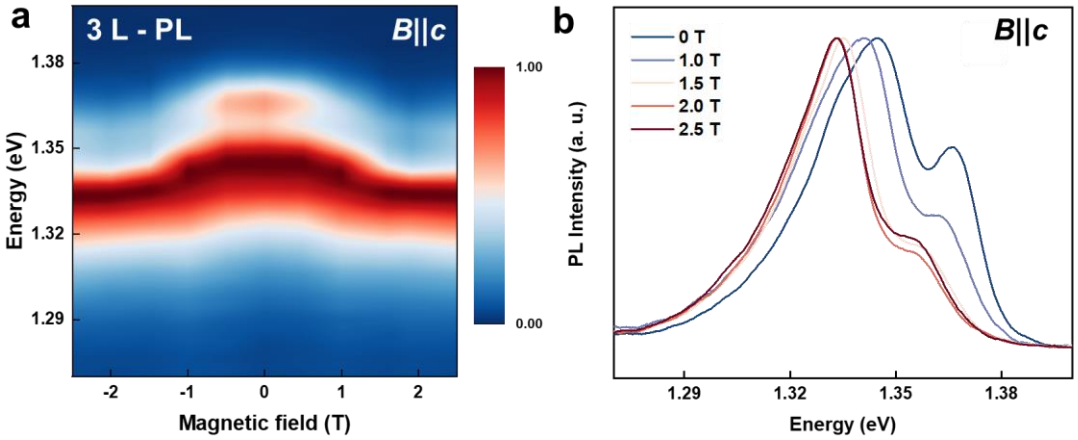

Figure S17. (a) PL spectra of 3-layer CrSBr as magnetic field is swept along the hard axis from -2.5 to 2.5 T. (b) PL spectra of 3-layer CrSBr under five different magnetic fields.

To quantify this intensity modulation, we also calculated the modulation efficiency η_{out} under B_{out}. When B_{out}. is increased from 0 T to 3 T, η_{out} reaches 73.8%. This higher value of η_{out} compared to η_{in} not only demonstrates the superior modulation efficiency achievable with B_{out} relative to B_{in} but also highlights the multidimensional magnetic controllability inherent in this device. This achievement signifies the

realization of direct manipulation of EL intensity via controlled spin transition. Our approach surpasses conventional LEDs relying on indirect spin manipulation methods, such as magnetic dopant incorporation or coupling to magnetic substrates[4-6]. Consequently, this device not only provides a novel prototype for electrically driven light emitters in opto-spintronic devices but also represents a significant step towards practical application with the large modulation efficiency η.

References

1 Sun, D. *et al.* Room-temperature magnetically modulated electroluminescence from hybrid organic/inorganic spintronics devices. *Appl. Phys. Lett.* **103** (2013).

2 Grünbaum, T. *et al.* Highly anisotropic magnetoresistance of organic light-emitting diodes at geomagnetic field strengths. *Phys. Rev. B* **108**, 035201 (2023).

3 Dorokhin, M. V. *et al.* Magnetically controlled spin light-emitting diode. *Uspekhi Fizicheskikh Nauk* **195**, 543-556 (2025).

4 Dang, J. *et al.* Electrical switching of spin-polarized light-emitting diodes based on a 2D CrI_3/hBN/WSe_2 heterostructure. *Nat. Commun.* **15**, 6799 (2024).

5 Li, J.-X. *et al.* Electric control of valley polarization in monolayer WSe_2 using a van der Waals magnet. *Nat. Nanotechnol.* **4**,1-8 (2022).

6 Ye, Y. *et al.* Electrical generation and control of the valley carriers in a monolayer transition metal dichalcogenide. *Nat. Nanotechnol.* **11**, 598-602, (2016).